Mutational analysis of active-site residues of the enterococcal D-Ala–D-Ala dipeptidase VanX and comparison with *Escherichia coli* D-Ala–D-Ala ligase and D-Ala–D-Ala carboxypeptidase VanY

Ivan AD Lessard and Christopher T Walsh

Background: Vancomycin-resistant enterococci are pathogenic bacteria that attenuate antibiotic sensitivity by producing peptidoglycan precursors that terminate in D-Ala–D-lactate rather than D-Ala–D-Ala. A key enzyme in effecting antibiotic resistance is the metallodipeptidase VanX, which reduces the cellular pool of the D-Ala–D-Ala dipeptide.

Results: We constructed eleven mutants, using the recently determined VanX structure as a basis, to investigate residue function. Mutating Asp142 or Ser114 showed a large effect principally on K_M, consistent with roles in recognition of the D-Ala–D-Ala termini. The drastic reduction or absence of activity in the Arg71 mutants correlates with a role in the stabilization of an anionic tetrahedral transition state. Three residues of the *Escherichia coli* D-Ala–D-Ala ligase (Ddl), Glu15, Ser 281 and Arg255, are similarly conserved and have equivalent functions with respect to VanX, consistent with a convergent evolution of active sites to bind D-Ala–D-Ala and lower energy barriers for formation of the tetrahedral intermediate and transition states. In the *N*-acyl-D-Ala–D-Ala carboxypeptidase VanY, all active-site residues are conserved (except for the two responsible for recognition of the dipeptide amino terminus).

Conclusions: The mutagenesis results support structure-based functional predictions and explain why the VanX dipeptidase and Ddl ligase show narrow specificity for the D,D-dipeptide substrate. The results reveal that VanX and Ddl, two enzymes that use the same substrate but proceed in opposite directions driven by distinct cofactors (zinc versus ATP), evolved similar architectural solutions to substrate recognition and catalysis acceleration. VanY sequence analysis predicts an active site and mechanism of reaction similar to VanX.

Address: Department of Biological Chemistry and Molecular Pharmacology, Harvard Medical School, Boston, MA 02115, USA.

Correspondence: Christopher T Walsh
E-mail: walsh@walsh.med.harvard.edu

Key words: D-Ala–D-Ala dipeptidase, DdlB ligase, mutagenesis, VanX, VanY

Received: **2 December 1998**
Revisions requested: **5 January 1999**
Revisions received: **13 January 1999**
Accepted: **13 January 1999**

Published: **22 February 1999**

Chemistry & Biology March 1999, 6:177–187
http://biomednet.com/elecref/1074552100600177

 ISSN 1074-5521

Introduction

The worldwide resurgence of infectious diseases, largely due to the appearance of antibiotic-resistant bacteria, is a serious medical problem [1–3]. Vancomycin-resistant enterococci (VRE) have become recognized as important opportunistic human pathogens over the past decade. Increased reliance on the glycopeptide antibiotic vancomycin to treat enterococcal infections and those caused by the dreaded methicillin-resistant *Staphylococcus aureus* (MRSA) [4] has not only caused a rise in clinically significant resistance and mortality from VRE, but also represents a looming infectious catastrophe for MRSA [4–8]. In the most prevalent clinical phenotypes of vancomycin resistance, VanA and VanB [8], bacteria have developed a strategy for reprogramming cell wall biosynthesis to new peptidoglycan precursor termini, which exhibit dramatically lower affinity for vancomycin. This paradigm of bacterial adaptation requires expression of the genes *vanR*, *vanS*, *vanH*, *vanA* and *vanX* (using VanA phenotypic nomenclature, Figure 1) [9] to produce peptidoglycan chain precursors terminating in D-alanyl–D-lactate (D-Ala–D-lactate) in place of D-alanyl–D-alanine (D-Ala–D-Ala), resulting in a 1000-fold decrease in vancomycin binding affinity and in unimpeded peptide strand cross-linking. The outcome is a mechanically strong cell wall whose synthesis is not inhibited by glycopeptides [10]. VanS and VanR act as a two-component regulatory system to mediate antibiotic-induced transcription of the genes *vanH*, *vanA* and *vanX*, whose products act sequentially (VanH, VanA) to synthesize the depsipeptide D–Ala–D–lactate in place of the normal D-Ala–D-Ala dipeptide [11,12]. VanX is a zinc-containing D,D-dipeptidase that hydrolyzes D-Ala–D-Ala but not D-Ala–D-lactate, allowing the D,D-depsipeptide to accumulate and become incorporated in the growing peptidoglycan termini [13,14]. In the VanA VRE phenotype, these genes are clustered on a transposon with two genes associated for transposition functions (*orf1* and *orf2*) and two other *van* genes, *vanY* and *vanZ* [9] (Figure 1). Although the VanY D,D-carboxypeptidase is not essential for a high level of resistance in the VanA VRE phenotype, it is believed to contribute moderately

Figure 1

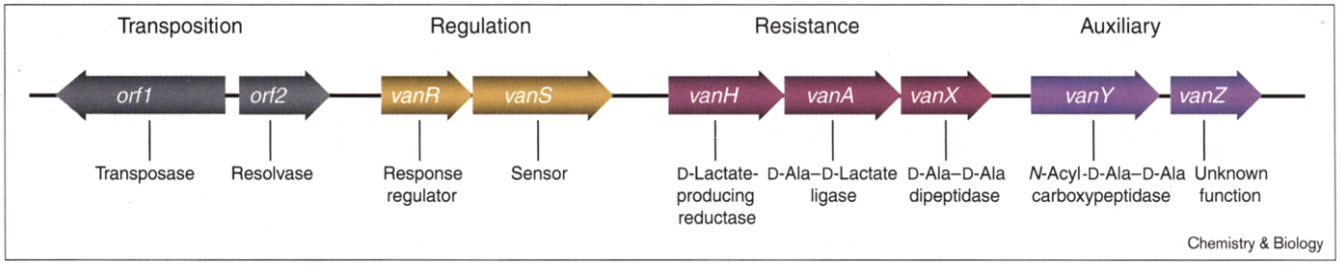

Schematic representation of the genes required for a high level of resistance to vancomycin in the VanA phenotype found within the transposon Tn*1546* [9]. The *vanR*, *vanS*, *vanH*, *vanA* and *vanX* genes are essential for a high level of resistance; the *vanY* and *vanZ* genes are nonessential. *orf1* and *orf2* encode proteins required for transposition.

to the resistance (e.g. in the VanB phenotype) by removing the terminal D-Ala from the newly synthesized UDP-muramyl-L-Ala–D-Glu–L-Lys–D-Ala–D-Ala that has escaped the VanX route [15]. *vanZ* has no identified function and it is not essential for resistance.

The origin of the glycopeptide resistance genes in enterococci has been an issue since their discovery; a first glimpse at a possible source came with the recent detection of a *vanHAX* gene cluster similar to that found in VRE in the glycopeptide antibiotic-producing *Streptomyces toyocaensis* and *Amycolatopsis orientalis* [16]. The demonstration that the VanX homolog (StoVanX) encoded by the *S. toyocaensis vanHAX* gene cluster possesses both the anticipated D-Ala–D-Ala dipeptidase activity and lacks D-Ala–D-lactate depsipeptidase activity [17] suggests a conserved mechanism for the observed intrinsic resistance of the antibiotic producers to the vancomycin class of glycopeptides. As *S. toyocaensis* also possesses a D-Ala–D-Ala ligase [18], the *vanHAX* genes may be switched on transcriptionally as the host commences antibiotic biosynthesis, allowing cell-wall termini to be reprogrammed to effect immunity to vancomycin in a timely fashion. Such a regulatory circuit (yet to be verified experimentally) is consistent with the view that antibiotic-resistance genes might have coevolved with the antibiotic-biosynthesis genes.

VanX homologs have also been detected in the gram-negative bacterium *Escherichia coli* (EcoVanX) and *Synechocystis* sp. (SynVanX), which have no need for defense against glycopeptide antibiotics (the outer membranes of *E. coli* and *Synechocystis* sp. are impermeable to vancomycin) [17]. In *E. coli*, the *ecovanX* gene is found clustered with a putative dipeptide permease system that permits import of D-Ala–D-Ala into the cell [17]. The consecutive action of *ecovanX*, pyruvate oxidase and the membraneous D-amino acid dehydrogenase would permit an energy generating role for this enzyme couple upon induction of the *ecovanX* and downstream permease genes by the stationary phase transcription factor σ^s under starvation conditions. A possible source of periplasmic D-Ala–D-Ala could be L,D-*meso*-diaminopimelic acid (A_2pm)–A_2pm transpeptidation, which increases during stationary phase [17].

VanX and D-Ala–D-Ala ligase (Ddl) catalyze antagonistic reactions — Ddl operates in the dipeptide biosynthetic direction, whereas VanX operates in the hydrolytic direction (Figure 2a). Because enzymes catalyze reactions in both directions (although the equilibria might be heavily biased in one direction, in this instance Ddl is driven in the contrathermodynamic direction by coupling ATP hydrolysis to amide-bond formation), the two opposing enzymes have many of the same requirements. In this case, they must recognize the ground state for D-Ala–D-Ala as substrate (VanX) or product (Ddl), and differentially recognize the two D-Ala monomers as electrophile and nucleophile (Ddl) or as first leaving group (VanX). Ddl and VanX must form and stabilize tetrahedral adducts at the amide link of D-Ala–D-Ala to lower activation barriers and speed up catalysis. To perform their related tasks, one enzyme uses ATP cleavage to drive amide-bond synthesis (Ddl), whereas the other employs zinc to activate bound water for hydrolysis of D-Ala–D-Ala (VanX). Despite the difference in cofactor usage, one might expect the catalytic inventory for the D-Ala–D-Ala ligase and the D-Ala–D-Ala dipeptidase active sites to be analogous and fulfill equivalent functions. To recognize D-Ala–D-Ala (as substrate or nascent product) one would expect an active-site residue in each enzyme to hydrogen bond and/or charge pair with the α-NH_3^+ of D-Ala–D-Ala (most likely Enz-COO^-) and a corresponding recognition of the substrate-COO^- to occur as well (Enz-OH utilized). To stabilize the incipient charge that develops in the transition state as the planar sp^2 carbonyl moiety is transformed to the sp^3 tetrahedral anion (and vice versa; Figure 2a) one would expect an enzyme active-site cation properly placed to stabilize the developing negative charge (e.g. a multidentate arginine-sidechain; Figure 2b).

The recent crystal structure determination of enterococcal VanX [19] and the existing X-ray structure of *E. coli* D-Ala–D-Ala ligase (DdlB) [20] with tetrahedral phosphinate transition-state analogs (Figure 3) as well as with substrate

Figure 2

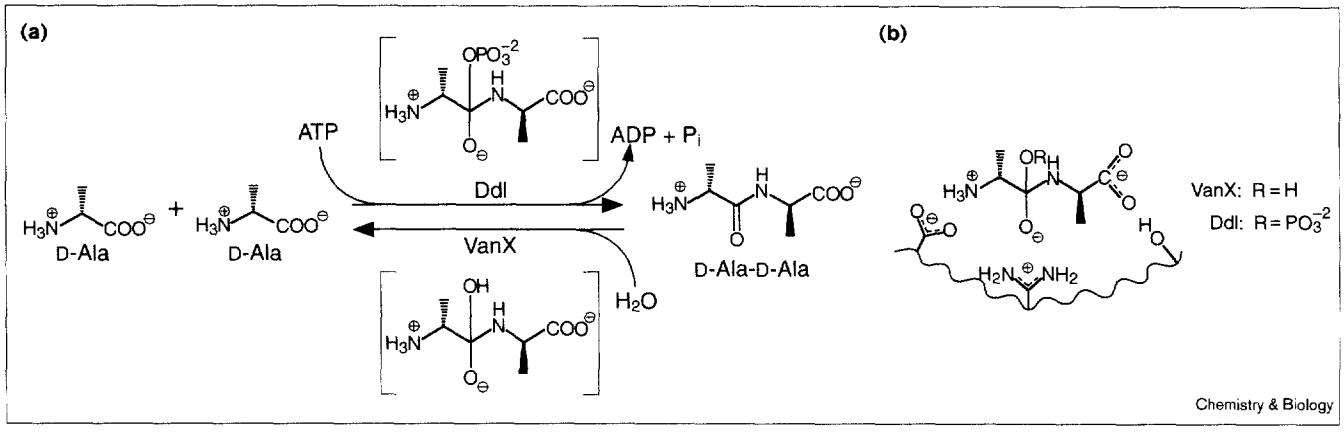

Reactions catalyzed by the Ddl and VanX enzymes. **(a)** DdlB and VanX catalyze antagonistic reactions. The Ddl ligase runs in the amide synthetic direction and has to consume a molecule of ATP to allow the reaction to proceed. In contrast, VanX runs in the hydrolytic direction and uses a zinc atom and a water molecule to accomplish its task. Both enzymes must form and stabilize similar tetrahedral adducts at the amide link of the D-Ala–D-Ala molecule, however. **(b)** Despite their difference in cofactor usage, similar sidechains between the two enzymes are predicted for ground state and specific binding, and transition-state stabilization.

for VanX, has given us a view of the active-site geometry and the disposition of active-site sidechains. The VanX structure, in particular, predicts specific enzyme sidechains that could fulfill the requirements shown in Figure 2 for both ground-state recognition and specific binding, as well as for transition-state stabilization. To test these predictions we have generated mutants of VanX at seven different positions and evaluated the catalytic efficiency of the mutant enzymes. We compare equivalent sidechain functions in Ddl. Sequence analysis of VanY and VanX, in addition to comparison with the X-ray structure of the zinc-dependent D-Ala–D-Ala carboxypeptidase (a VanY homolog) from *Streptomyces albus* G (Ddp) [21], has allowed us to predict an equivalent organization of the active sites of these enzymes for recognition and hydrolysis of either the *N*-acyl-D–Ala-D-Ala (VanY and Ddp) or D-Ala–D-Ala (VanX).

Results

Design and production of VanX mutants

The recently reported X-ray structure of enterococcal VanX [19] bound to its substrate D-Ala–D-Ala and phosphinate, a reaction intermediate analog [22], guided the initial mutant construction design to test for residue function. At the amino terminus of bound D-Ala–D-Ala or phosphinate, three VanX residues (Tyr21, Asp142 and Asp123) were found in close proximity for hydrogen bonding with the substrate/analog α-NH_3^+ (Figures 3 and 4). Asp123 was shown previously to be a critical ligand for zinc binding [23]. Tyr21 was mutated to phenylalanine and Asp142 to an alanine or asparagine residue. Ser115 has been proposed to form a hydrogen bond at the carboxyl end of bound D-Ala–D-Ala, whereas it is the sidechain of Ser114 that appears to play this role in the case of bound phosphinate. Both Ser114 and Ser115 were changed singly to alanine. Arg71 is a candidate to stabilize the anionic tetrahedral adduct and its associated transition states so it was mutated to an alanine, histidine or lysine residue. Tyr35 and Asp68 are in position to form a hydrogen-bond triad with Arg71 and could serve to orient Arg71. Tyr35 was mutated to phenylalanine and Asp68 to alanine or asparagine. We showed previously that VanX retains full activity as a D,D-dipeptidase when fused to maltose-binding protein (MBP) [23], so the kinetic data reported in Table 1 were obtained using the intact MBP–VanX mutant fusion proteins in each case.

Characterization of MBP–VanX mutants as D-Ala–D-Ala dipeptidases

Table 1 lists the steady-state kinetic data of various MBP–VanX mutants. For a zinc-dependent peptide-bond hydrolase such as VanX, catalytic efficiency will be determined by optimizing the orientation of the substrate D-Ala–D-Ala and water as ligands at or around the catalytic zinc and lowering barriers for reaction. Coordination of the substrate D-Ala–D-Ala and the tetrahedral adduct to zinc are anticipated and supported by the X-ray data [19]. Three categories of effects were observed for the VanX mutants: modest change: Tyr21→Phe, Tyr35→Phe and Ser115→Ala; intermediate change: Ser114→Ala; and large change: the Asp142, Arg71 and Asp68 mutants.

Modest effects: Tyr21→Phe, Tyr35→Phe and Ser115→Ala

The mutant Tyr21→Phe is only decreased 125-fold in catalytic efficiency (k_{cat}/K_M), which mainly results from a 38-fold increase in K_M. The loss of the phenolic hydroxyl,

Figure 3

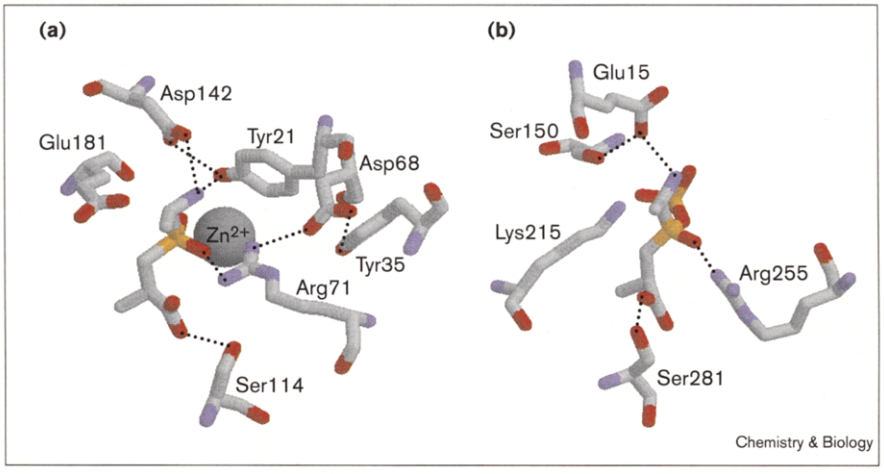

Crystal structure comparison of the active-site residues of **(a)** VanX and **(b)** DdlB with bound phosphinate [19] and phosphorylphosphinate [20], respectively. Glu15, Ser281 and Arg255 in DdlB are similarly placed with respect to the transition-state analog and are functionally equivalent to Asp142, Ser114 and Arg71 in VanX. Ser150 orients Glu15 in DdlB as Tyr21 orients Asp142 in VanX. Tyr21 is also hydrogen bonded to the substrate α-NH_3^+. The arginine residues stabilize the transition-state intermediate with help from Lys215 in DdlB and the zinc atom in VanX. Arg71 in VanX is oriented by Asp68 and Tyr35. DdlB uses Lys215 for phosphate transfer, whereas VanX uses the similarly placed Glu181 to abstract a proton from a water molecule for subsequent attack on the carbonyl group of the substrate. The zinc ligands are His116, Asp123 and His184.

abrogating a medium-length hydrogen bond (3.2 Å) to the α-NH_3^+ group of the dipeptide has only a modest effect, suggesting that this is not a crucial interaction by itself.

The second tyrosine residue, Tyr35, is part of a triad with the Arg71 and Asp68 residues that probably form hydrogen bonds with each other to orient the guanidinium sidechain of Arg71 to stabilize the incipient negative charge of the tetrahedral transition state after the attack of the zinc-coordinated water molecule (Figure 4). Disruption of Tyr35 hydrogen-bonding potential (Tyr35→Phe) is noticeable but slight (there is a 21-fold increase in K_M).

Figure 4

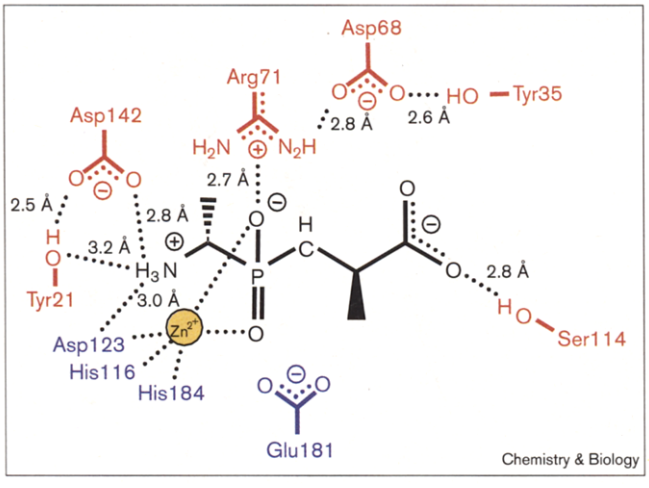

Schematic diagram of the active-site residues in the enterococcal VanX complexed with the phosphinate transition-state analog. Possible interactions are shown by dashed lines. Hydrogen bond distances are indicated. The residues colored blue were investigated previously [23]. The residues colored red were investigated in this study.

The Asp68 sidechain is probably the primary determinant controlling the orientation of Arg71 (see below).

The Ser115→Ala mutation has a very small effect. The K_M increases by a factor of two but because the k_{cat} increases threefold, the mutant is actually a better catalyst than wild-type VanX. This result turns out not to be so surprising because this residue is not conserved in other VanX homologs (except for the VanX from the type B resistance) [17]. Ser115 is, therefore, not a crucial substrate-binding element and the Ser115→Ala mutant serves as a good control for interpreting the Ser114→Ala mutant.

Intermediate effect: Ser114→Ala

The Ser114→Ala mutant is a 2500-fold less efficient enzyme with only a 1.2-fold decrease in k_{cat} but a 2000-fold increase in K_M. The loss of enzyme efficiency is entirely due to loss of substrate binding, as would be expected for a ground-state effect in substrate COO^- recognition. The element for binding of the carboxylate end of the substrate is therefore Ser114 as observed in the VanX structure with bound phosphinate and not Ser115 as was observed with bound D-Ala–D-Ala [19].

Large effects: Arg71, Asp142 and Asp68 mutants

Arg71→Ala and Arg71→His mutants show no detectable dipeptidase activity over a time course of 12 h, suggesting that Arg71 is crucial. The Arg71→Lys mutant has detectable activity but shows a 1.7×10^6-fold decrease in catalytic efficiency, due to a 2750-fold increase in K_M and a 670-fold reduction in k_{cat}. These results suggest substantial loss of transition-state recognition/stabilization. The Arg71 mutants are most seriously affected, consistent with a key role in catalytic function. Neither the Arg71→Lys nor the Arg71→His basic sidechains seem to be able to achieve an orientation that can substitute for the placement of Arg71.

Table 1

Kinetic parameters of purified MBP-VanX mutants fusion proteins using D-Ala-D-Ala as substrate.

Protein	k_{cat} (s^{-1})*	Decrease (x-fold)	K_M (mM)	Increase (x-fold)	k_{cat}/K_M ($s^{-1}mM^{-1}$)	Decrease (x-fold)
Wild type	26	–	0.080	–	330	–
Tyr21→Phe	7.8	3	3.0	38	2.6	125
Asp142→Ala	0.037	703	6.5	81	0.0056	58000
Asp142→Asn	0.30	87	96	1200	0.0031	105000
Ser114→Ala	22	1.2	160	2000	0.13	2500
Ser115→Ala	73	0.36	0.16	2	460	0.71
Arg71→Ala	nd	–	nd	–	nd	–
Arg71→His	nd	–	nd	–	nd	–
Arg71→Lys	0.041	634	220	2750	0.00019	1700000
Asp68→Ala	0.097	270	60	750	0.0016	200000
Asp68→Asn	0.12	217	5.0	63	0.024	14000
Tyr35→Phe	10	2.6	1.7	21	5.8	56

MBP–VanX samples were prepared from cells grown in LB media supplemented with 200 μM $ZnSO_4$. *Dipeptidase activity was assayed by measuring the production of D-Ala using the modified cadmium–ninhydrin method (see the Materials and methods section). Protein concentrations were determined from the corrected absorbance at 280 nm in H_2O [40]. nd, no detectable activity over 12 h.

The Arg142→Ala and Arg142→Asn mutants were constructed because the X-ray structure of VanX shows that Asp142 is within 2.8 Å of the D,D-substrate's α-NH_3^+, consistent with participation in ground-state recognition (Figure 4). The Asp142→Asn mutant is decreased only 87-fold in k_{cat} but is increased 1200-fold in K_M, suggesting that Asn142 might still be able to hydrogen bond with the D,D-substrate α-NH_3^+. The k_{cat} of the Asp142→Ala mutant is decreased 700-fold, an order of magnitude worse than the Asp142→Asn mutant. It is not clear why the K_M is only increased 81-fold, however. These effects in k_{cat} and K_M have not been subdivided into effects on microscopic rate constants, so we make no further interpretation about effects on elementary steps.

When the importance of Asp68 was examined, with the Asp68→Asn and Asp68→Ala mutants, substitution of aspartate by asparagine preserves more function than the aspartate to alanine switch. Here, both mutants have a 200–300-fold decrease in k_{cat} but the Asp68→Asn mutant only has a 63-fold increase in K_M, whereas in the Asp68→Ala mutant, the K_M was 750-fold worse. The VanX crystal structure shows that Asp68 is the central residue in the Arg71–Asp68–Tyr35 hydrogen-bonding triad. Presumably the asparagine sidechain in the Asp68→Asn mutant retains more contact with Arg71 than does the alanine sidechain in the Asp68→Ala mutant, assisting in productive orientation of Arg71 for transition-state stabilization.

Detection of novel activity in mutant proteins

We examined the mutant proteins for 'gain of function' novel activities by testing other potential enzyme substrates. In no case was *N*-acetyl-D-Ala–D-Ala a substrate, even for the Tyr21→Phe mutant, but the reverse regioisomer of D-Ala–D-lactate, the D-lactyl–D-Ala amide (which lacks an α-NH_3^+ group) showed an interesting substrate profile. Three mutants, Asp142→Ala, Asp142→Asn and Tyr21→Phe, had an increased ability to hydrolyze D-lactyl–D-Ala. The Asp142→Asn and Asp142→Ala mutants showed a 60- and 160-fold increase in peptidase activity, respectively, compared with the wild-type enzyme, which has a barely detectable k_{cat}/K_M of 2×10^{-5} $mM^{-1}s^{-1}$, a factor of 10^7 worse than for D-Ala–D-Ala (Table 2). The Tyr21→Phe VanX mutant shows a much larger effect with an increase of 4300-fold in catalytic efficiency over the wild-type enzyme. For this mutant, D-Ala–D-Ala is only 30-fold better by k_{cat}/K_M criterion than D-lactyl–D-Ala. This 30-fold difference is almost entirely due to K_M. The k_{cat} of Tyr21→Phe for D-lactyl–D-Ala cleavage is only sixfold lower than the wild-type enzyme for its natural substrate, D-Ala–D-Ala, suggesting a similar substrate orientation for peptide cleavage in each enzyme. In wild-type VanX Tyr21, which hydrogen bonds to Asp142, might exclude D-lactyl–D-Ala by means of electrostatic repulsion between two oxygens. The Asp142 mutants have only a twofold increase in catalytic efficiency for D-Ala–D-Ala than D-lactyl–D-Ala. Again removal of electron density close to the binding site for D-Ala–D-Ala α-NH_3^+ allows better binding of the uncharged D-lactyl–D-Ala substrate. Interestingly, in DdlB, a D-lactyl–D-Ala ligase activity was detected in the Glu15→Gln mutant [24]. Both Glu15 in DdlB and Asp142 in VanX are involved in the α-NH_3^+ recognition of the substrate D-Ala for DdlB and D-Ala–D-Ala for VanX.

Discussion

Metalloproteases have been a successfully targeted for rationally designed therapeutic agents in other biological contexts (e.g. angiotensin converting enzyme inhibitors), suggesting that VanX is a prime candidate for design of inhibitors to combat VRE. In an earlier study of the zinc-dependent metallodipeptidase enterococcal VanX (VanA-type resistance), we identified, using mutagenesis, residues His116, Asp123 and His184 as probable zinc-coordination

Table 2

Kinetic parameters of purified MBP-VanX mutants fusion proteins using D-lactyl-D-Ala as substrate.

Protein	k_{cat} (s^{-1})*	K_M (mM)	k_{cat}/K_M ($s^{-1}mM^{-1}$)	Increase (x-fold)
Wild type	ns	ns	0.000021	-
Tyr21→Phe	4.3	47	0.091	4300
Asp142→Ala	0.066	20	0.0033	160
Asp142→Asn	0.18	150	0.0012	60

*See comments in Table 1. ns, no saturation.

ligands and Glu181 as the probable general base for deprotonation of the zinc-coordinated water molecule that subsequently attacks the D-Ala–D-Ala substrate [23]. The recent crystallographic structure determination of enterococcal VanX has confirmed these assignments [19].

Similar recognition features for D-Ala–D-Ala ligase and D-Ala–D-Ala dipeptidase

A comparison of the active-site organization for substrate and transition-state recognition by the ligase Ddl and the hydrolase VanX has been enabled by X-ray structures with tightly binding inhibitors, phosphinate for VanX and phosphorylated phosphinate for Ddl, that built on our earlier mechanistic studies of each enzyme [22,25]. The bound phosphinate ligands in each enzyme are taken to be stable analogs of the two tetrahedral intermediates (Figure 2a) and so have suggested orientations of the corresponding reaction intermediate in the active site of each enzyme. Figure 3 shows a remarkable correspondence of orientation of the same three types of sidechains for the same three functions in the ligase and dipeptidase active site: Glu15 (Ddl) versus Asp142 (VanX) for hydrogen bonding/charge pairing to the positively charged amino group of tetrahedral adduct phosphinate analogs; Ser281 (Ddl) versus Ser114 (VanX) for equivalent hydrogen bonds to the carboxyl end of the D,D-analog; and Arg255 (Ddl) versus Arg71 (VanX) for binding to the tetrahedral phosphinate oxygen (analagous to the tetrahedral adduct of the substrate) for transition-state/tetrahedral-adduct stabilization. In Ddl, Glu15 is oriented by Ser150 and Tyr216 in a hydrogen-bond network. In VanX Asp142 is similarly oriented by Tyr21. Mutation of either Ser150 or Tyr216 in Ddl [25] or Tyr21 in VanX, has only modest effects on catalytic efficiency. In contrast, mutation of Glu15 in Ddl [25] or Asp142 in VanX has a pronounced effect on catalytic activity. Mutations at Ser281 in Ddl [25] or Ser114 in VanX also have a substantial effect on substrate recognition as predicted. The Arg255→Ala Ddl mutant experienced at least a 2000-fold decrease in k_{cat}, at the noise level of the assay [25], which parallels the crucial role of Arg71 demonstrated here for VanX catalysis.

It appears that a parallel strategy evolved in these otherwise quite different enzymes to provide, first, a specific binding pocket that recognizes only the unmodified D,D-dipeptide and, second, to stabilize developing anionic charge arising from rehybridization of the substrate amide carbonyl in the tetrahedral adduct. The other elements of the catalytic apparatus of each enzyme have evolved differently. The ligase runs in the amide synthesis direction and requires hydrolysis of one molecule of ATP to drive that equilibrium, mechanistically activating the γ-phosphoryl for attack by the first D-Ala (Figure 2a). The Lys215 of Ddl is required to act as a charge shield for the negative charge on the γP of ATP to lower electrostatic repulsions in the catalytic instant of phosphoryl transfer. No such function exists in VanX and there is no equivalent residue. There is, instead, a zinc atom in the VanX active site poised to interact with the bound substrate's dipeptide carbonyl group and to coordinate a water molecule that will attack the amide bond. VanX needs a general base to activate the zinc–water complex, a function that is provided by Glu181 (Figure 3). There is no comparable requirement in Ddl and therefore no comparable general base. The polarity of Lys215 in Ddl (cationic) and Glu181 in VanX (anionic) is therefore reserved for the two specific and differentiated jobs that these opposing enzymes have to perform.

VanY and Ddp: two *N*-acyl-D-Ala–D-Ala carboxypeptidases with similar active-site residues equivalent to VanX

The identification of residues for zinc coordination in the VanX enzyme has revealed a new family of zinc proteases that uses the novel consensus sequence SxHxxGxAxD, where aspartate and histidine residues are zinc ligands (the third and fourth ligands to zinc are a histidine several residues downstream in the primary sequence and water) [23]. The VanY and Ddp enzymes both have this consensus 'zinc motif' [23] (although the VanY has yet to be validated for zinc content, its activity was shown to be dependent on divalent ions [26]) and act analogously on D-Ala–D-Ala peptides as carboxypeptidases. VanY and Ddp differ from VanX in that they act on *N*-acylated-D,D-peptide, and VanY shows activity towards the depsipeptide *N*-acyl-D-Ala–D-lactate [27]. Structural comparison of VanX and Ddp revealed a strong homology in and around the active site [19]. The zinc ligands, the serine residue for recognition of the terminal carboxylate moiety of D-Ala–D-Ala and the arginine residue for stabilization of the transition state are structurally conserved in Ddp and VanX (Figure 5a). In Ddp a histidine residue apparently replaces Glu181 of VanX as catalytic base for water activation. The overall root mean square deviation value for superimposition of the sidechains of the zinc ligands, glutamate/histidine, serine and arginine residues is 1.03 Å. The key Asp68–Arg71 hydrogen bond interaction of VanX is mimicked by an Arg138–Asn143 interaction in Ddp.

Primary sequence analysis suggests that the two enterococcal proteins VanY and VanX are more closely related than Ddp is to either VanX or VanY. We predicted previously

Figure 5

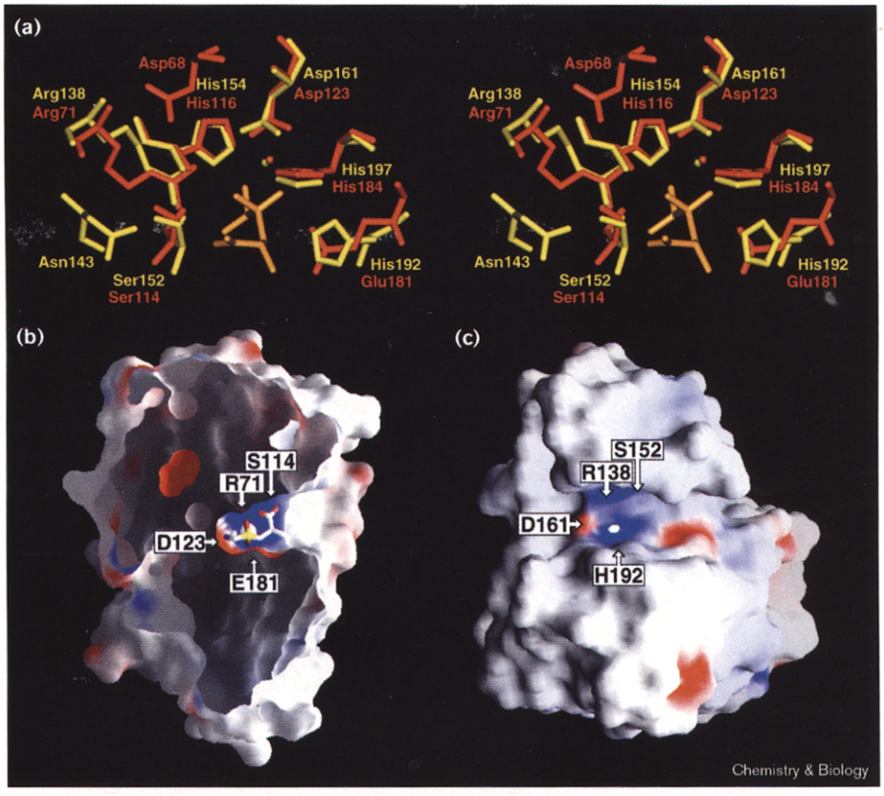

Structural comparison of the active-site arrangements of VanX with bound phosphinate with Ddp. **(a)** Stereo diagram of the structural alignments of active-site residues of VanX (red) and Ddp (yellow). The zinc atoms are shown in red (VanX) and yellow (Ddp) and the phosphinate bound to VanX is orange. The alignment was performed on the sidechains shown, except for Asp68 (VanX) and Asn143 (Ddp), using the program Quanta® (Molecular Simulations Inc.). **(b)** VanX and **(c)** Ddp surface electrostatic potential representation. Both proteins are positioned so that the conserved active-site residues highlighted in (a) are similarly oriented. The Ddp active site forms a channel on the surface. The VanX active site is in a pocket. The view of VanX has been cut away to reveal the active site and the bound phosphinate. The position of the active-site residue arginine (transition-state stabilization), aspartate (zinc ligand), serine (carboxylate recognition) and glutamate/histidine (catalytic base) are indicated by arrow boxes using single-letter amino-acid code. The position of the other two zinc ligands (histidine residues) is approximated by the blue color surrounding the zinc atom (white), which is partially buried in both structures. The calculations were performed using GRASP [43] with a water probe radius of 1.4 Å and electrostatic potential ranging from blue (+50 kt/e) to red (−50 kt/e).

the catalytic glutamate residue (Glu238) and zinc ligands (His188, Asp195 and His241) for the enterococcal VanY [23] (Figure 6). A BLAST search (http://www.ncbi.nlm.nih.gov/) detected seven additional bacterial homologs to VanY, including VanY from the VanB VRE phenotype (but did not rank Ddp as a homolog), and has allowed us to identify potential active-site residues. In all cases the Arg–(Asn/Gln) pair is conserved, which is indicative of a similar role for the arginine of VanY in transition-state stabilization. Another similarity is the conservation of the equivalent of the VanX active site Trp197 [19] in all VanY and VanX homologs in an E(P/W)WH motif. This tryptophan residue is found in proximity to and is believed to interact with the transition-state adduct [19]. The serine residue just upstream of the first histidine ligand to zinc (SxHxxGxAxD), Ser186 in VanY, is strictly conserved in the VanY family and predicted to be structurally equivalent to Ser114 in VanX or Ser152 in Ddp. This serine is functionally responsible for recognition of the terminal carboxylate moiety of the muramyl-L-Ala–D-Glu–L-Lys–D-Ala–D-Ala substrate (Figure 6). The question arises, given the highly conserved architecture of active-site residues in VanX and VanY zinc carboxypeptidases (Figure 6) as to how the differential recognition of a free amino group (as in VanX) versus an *N*-acyl amino group (as in VanY) is achieved when scanning potential D-Ala–D-Ala substrates. The Tyr21 and Asp142 residues that recognize the α-NH_3^+ group in free D-Ala–D-Ala are not preserved in the VanY sequences. Their absence in the Ddp structure provides a channel for accommodation of an *N*-acyl chain that would be blocked off in VanX (Figure 5b,c). Aside from the residues highlighted in Figure 6, VanY and VanX show very little sequence homology, perhaps suggesting convergent evolution to a common catalytic geometry for binding and hydrolysis of the D,D-dipeptide moiety. Our analysis predicts that phosphinates will be potent inhibitors of VanY and might act synergistically with VanX inhibitors, but does not yet indicate why VanY (but not VanX) has detectable D,D-depsipeptide hydrolase activity. The homology between the VanY homologs outside the sequences highlighted in Figure 6 is very low.

Reaction mechanism of D,D-peptidase

The reaction mechanism of zinc proteases has been thoroughly investigated for thermolysin [28–30] and carboxypeptidase A enzymes [31,32] as representative zinc proteases (see [33] for review). Two variations for zinc-centered mechanisms have been proposed: the zinc hydroxide and the reverse protonation mechanisms (see [33] for review). In the zinc-hydroxide mechanism, the zinc ion functions in two ways; it polarizes the substrate carbonyl group and facilitates deprotonation of the bound water nucleophile [33]. A proximal sidechain carboxylate group shuttles a proton from the zinc-bound water nucleophile to

Figure 6

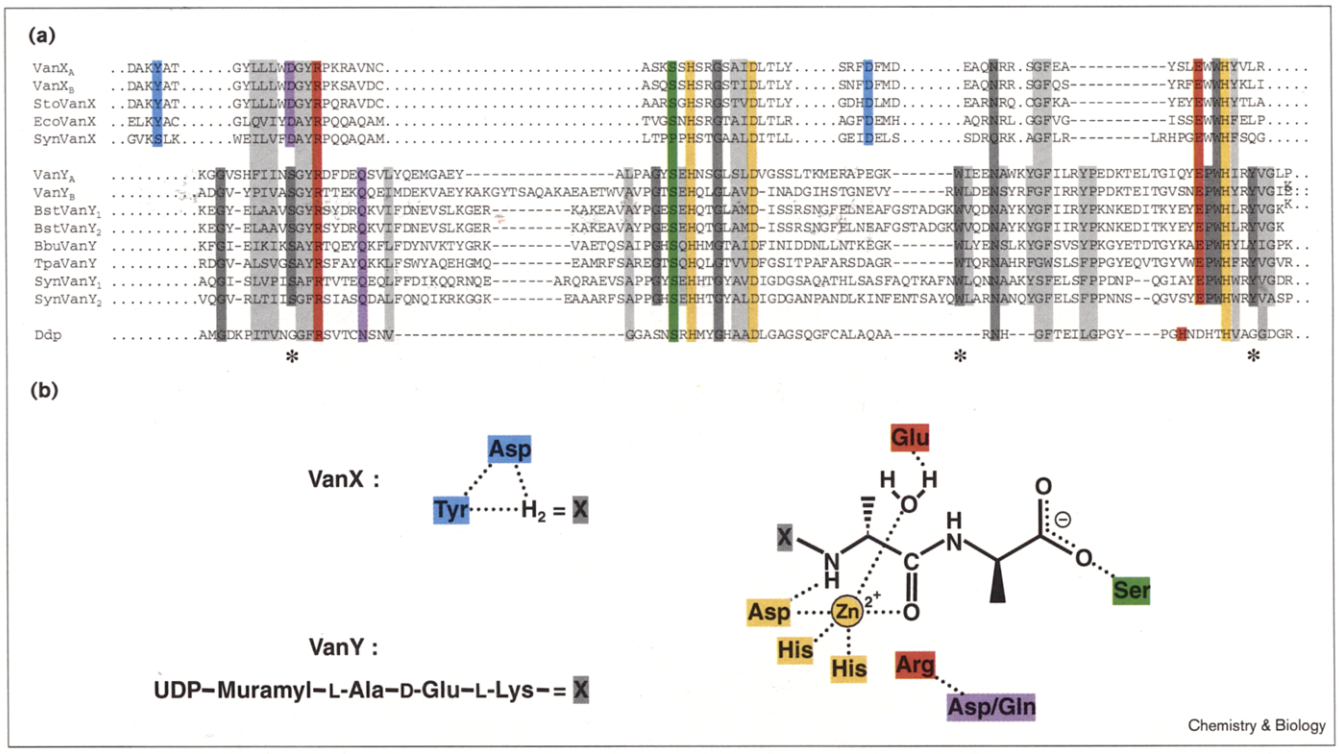

(a) Sequence alignment of VanY and VanX homologs and Ddp around the active-site residues. $VanX_A$, *Enterococcus faecium* VanX; $VanX_B$, *E. faecalis* VanX homolog; StoVanX, *Streptomyces toyocaensis* VanX homolog; EcoVanX, *Escherichia coli* VanX homolog; SynVanX, *Synechocystis* sp. PCC6803 VanX homolog; $VanY_A$, *E. faecium* VanY; $VanY_B$, *E. faecalis* VanY homolog; $BstVanY_1$, first *Bacillus subtilis* VanY homolog; $BstVanY_2$, second *B. subtilis* VanY homolog; BbuVanY, *Borrelia burgdorferi* VanY homolog; TpaVanY, *Treponema pallidum* VanY homolog; $SynVanY_1$, first *Synechocystis* sp. PCC6803 VanY homolog; $SynVanY_2$, second *Synechocystis* sp. PCC6803 VanY homolog; Ddp, *Streptomyces albus* G D-Ala–D-Ala carboxypeptidase. Identity and similarity are denoted by dark and light gray background. The zinc ligands are yellow, the catalytic base (glutamine/histidine) and transition-state residues (arginine) are red, the carboxylate-end-binding residue is green, the arginine-orientation residues are purple and the α-NH_3^+-binding residues are blue; all are shown in **(b)** the schematic diagram. The asterisk indicates potential functional residues required to recognize the extended substrate in the VanY family (serine, tryptophan and tyrosine residues). The alignment was performed using the CLUSTAL W method [44] on the entire VanY homolog sequences. The sequence of Ddp was aligned manually. The VanX sequence alignment has been published previously [17].

the leaving group. In contrast, the reverse protonation mechanism suggests that the zinc-bound water ligand will have to be protonated in order to be replaced by the carbonyl group of the substrate [30]. In this case, the conserved carboxylate-containing residue would play only a charge-neutralization role [32]. In thermolysin, a histidine residue would act as general base to activate the water nucleophile, whereas in carboxypeptidase A, this role would be played by the carboxylate group of the substrate [30,32].

The active-site architecture of a VanX–D-Ala–D-Ala enzyme complex is closer to that of carboxypeptidase A than thermolysin, by having a free carboxylate group of the substrate in proximity to the cleavage site and also the tetrahedral intermediate-stabilizing arginine residue (Arg71). In thermolysin, the arginine residue is replaced by tyrosine and histidine residues and there is no substrate carboxylate group near the cleavage site. In the cocrystal structures of VanX and phosphinate or D-Ala–D-Ala, there is no residue within 8.0 Å of the phosphinyl or carbonyl group that could deprotonate the water nucleophile other than Glu181 (3.3 Å; absolutely required for catalysis [23]) and the carboxylate group of the substrate (3.3 Å), favoring the zinc-hydroxide mechanism (Figure 7). Furthermore this residue is totally conserved in all VanX homologs identified to date [17]. In the present work we show that the Ser114 sidechain plays an important role in substrate recognition given the 2000-fold increase in K_M in the Ser114→Ala mutant. For a reverse-protonation mechanism involving the carboxylate group of the D-Ala–D-Ala substrate as the catalytic base such as has been proposed for the carboxypeptidase A [32], one would expect both kinetic parameters (not just on K_M) to be affected in the Ser114→Ala mutant. The overall conservation of critical residues for recognition and catalytic activity between VanX, VanY and Ddp suggest a similar reaction mechanism for these enzymes as well.

Figure 7

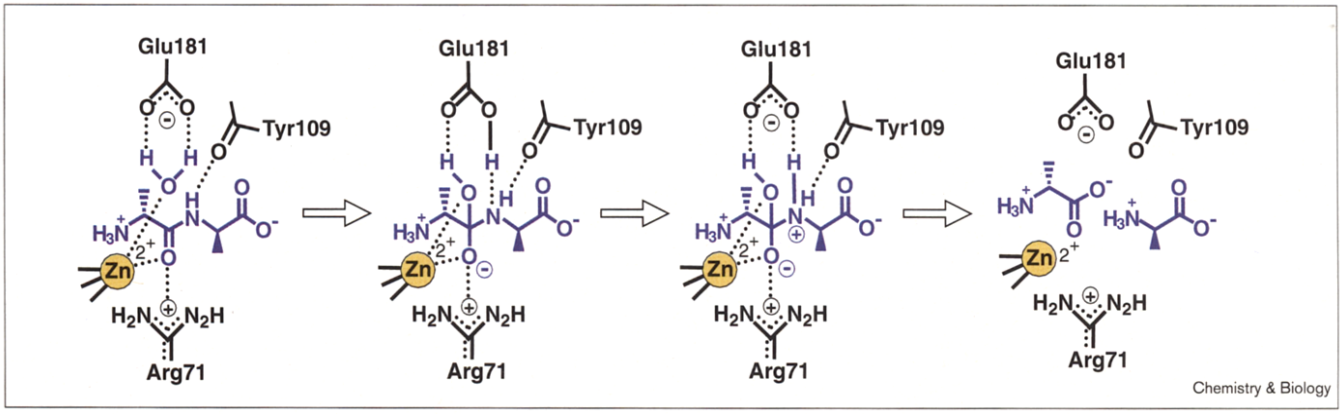

Proposed mechanism of VanX. The water molecule is activated by Glu181 and attacks the zinc-polarized carbonyl to form a tetrahedral intermediate stabilized by both the zinc atom and Arg71. Glu181 transfers the proton to the nitrogen that is hydrogen bonded to the carbonyl group of Tyr109; peptide-bond cleavage follows. A similar reaction mechanism has been proposed for thermolysin [28] and carboxypeptidase A [31].

Significance

The metallodipeptidase VanX plays an essential role in pathogenic vancomycin-resistant enterococci (VRE) by selectively depleting the cellular pool of D-Ala–D-Ala over D-Ala–D-lactate during reprogramming of cell wall biosynthesis to new peptidoglycan precursors terminating in D-Ala–D-lactate. There has been substantial interest in deciphering the mechanism, substrate specificity and three-dimensional structure of VanX, given that metalloproteases operating in other biological contexts, such as angiotensin converting enzyme have been successfully targeted for therapeutic intervention. We report here results from mutagenesis studies that support structure-based functional predictions and explain why the VanX dipeptidase and Ddl ligase enzymes show dramatic specificity for the small D,D-dipeptide substrate. The compact active sites and strict discrimination for small substrate ligands put constraints on inhibitor development for both VanX and the D-,D-ligase Ddl and the VRE D-,D-ligase counterpart VanA. This work shows similar architectural solutions to substrate recognition and acceleration of catalysis by two enzymes that use the same substrate but run in different directions driven by distinct cofactors (zinc versus ATP). We also identify conserved active-site residues in the VRE D-Ala–D-Ala carboxypeptidase VanY that predict a similar reaction mechanism and catalytic architecture to the VanX enzyme.

Materials and methods

Materials

Bacteriological media were obtained from Difco Laboratories. The competent *E. coli* strain BL21 (DE3) [F^-, *ompT*, *hsdS*$_B$, (r_{B-},m_{B-}), *gal*, *dcm*, (DE3)] was purchased from Novagen. Competent *E. coli* strain DH5α [F^-, ϕ80d*lac*ZΔM15, Δ(*lac*ZYA-*arg*F)U169, *deo*R, *rec*A1, *end*A1, *hsd*R17(r^{K-}, m^{K+}), *pho*A, *sup*E44, γ$^-$, *thi*-1, *gyr*A96, *rel*A1] was purchased from GibcoBRL. Restriction endonucleases, T4 DNA ligase, calf intestinal alkaline phosphatase, and amylose resin were obtained from New England Biolabs. *Pfu* DNA polymerase was purchased from Stratagene. Isopropyl-1-thio-β-D-galactopyranoside (IPTG) was purchased from Bachem Biosciences. Kanamycin, D-Ala–D-Ala and *N*-acetyl-D–Ala-D-Ala were purchased from Sigma. D-lactyl–D-Ala has been synthesized previously in this laboratory [24]. Chelex-100 resin and low molecular weight markers for polyacrylamide gel electrophoresis (PAGE) were obtained from Bio-Rad. Plasmid pIADL14 expressing the *vanX* gene from type A vancomycin resistant enterococci has been described previously [23].

Recombinant DNA methods

Recombinant DNA techniques were performed as described elsewhere [34]. Preparation of plasmid DNA, gel purification of DNA fragments, and purification of polymerase chain reaction (PCR)-amplified DNA fragments [35,36] were performed using the QIAprep® spin plasmid miniprep kit, QIAEX® II gel extraction kit and QIAquick™ PCR purification kit, respectively (QIAGEN). PCRs were carried out as described by Lessard and Perham [37], using the *pfu* DNA polymerase. Splicing by overlap extension (SOE) reactions [38] were carried out as for the PCR using approximately an equimolar ratio (total amount ~50 ng) of each of the gel-purified PCR-amplified DNA fragments to be joined as template. The fidelity of the SOE- or PCR-amplified DNA fragments was established by nucleotide sequencing after subcloning into the expression vector. Oligonucleotide primers were obtained from Integrated DNA Technologies, and DNA sequencing was performed on double-stranded DNA by the Molecular Biology Core Facility of the Dana Farber Cancer Institute (Boston, MA).

Site-directed mutagenesis

Site-directed mutants Ser114→Ala and Ser115→Ala were constructed from a pIADL14 template by PCR mutagenesis using the primer pairs 2044/1134 and 2044/1136, respectively (Table 3). The purified PCR-amplified DNA fragments were digested with *Nde*I and *Sac*II, gel-purified and subcloned into pIADL14. Site-directed mutants Tyr21→Phe, Tyr35→Phe, Asp68→Ala, Asp68→Asn, Arg71→Ala, Arg71→His, Arg71→Lys, Asp142→Ala and Asp142→Asn were constructed using the SOE method. In the first round of PCR, the sequences upstream and downstream of the mutation were amplified separately using a pIADL14 plasmid template and the primer pairs 2044/11XX and 21XX/1101, respectively, for all mutants except for the Asp142 mutants, which were amplified using the primer pairs 2001/11XX and 21XX/RSRP, respectively (Table 3; each mutant corresponds to a particular XX pair of

Table 3

Oligonucleotide primers for site-directed mutagenesis.

Comment	Code	5′–3′ Nucleotide sequence
MBP_{IntF}	2044	CCTGAAAGACGCGCAGACTAATTCG
$VanX_{IntRD145A}$	1101	AGAGCGTTCA***G***CCATAAAATCAAATC
$VanX_{IntF}$	2001	ACTGTTTTATGCAATGGGCTGC
$T7_{term}$	RSRP	CGTGAACCATCACCCTAATCAAG
Tyr21→Phe	2126	GGACGCTAAAT***T***TGCCACTTGG
Tyr21→Phe	1126	CCAAGTGGCA***A***ATTTAGCGTCC
Tyr35→Phe	2127	GGTTGACGGTT***T***TGAAGTAAATCG
Tyr35→Phe	1127	CGATTTACTTCA***A***AACCGTCAACC
Asp68→Ala	2122	GCTTCTATGGG***CA***GGTTACCGTCCTAAGC
Asp68→Ala	1122	GGACGGTAACC***TG***CCCATAGAAGCAATCC
Asp68→Asn	2123	GCTTCTATGG***A***ACGGTTACCGTCCTAAGC
Asp68→Asn	1123	GGACGGTAACCGT***T***CCATAGAAGCAATCC
Arg71→Ala	2128	GGACGGTTAC***GC***TCCTAAGCGTGC
Arg71→Ala	1128	GCACGCTTAGGA***GC***GTAACCGTCCC
Arg71→His	2129	GGACGGTTACC***A***TCCTAAGCGTG
Arg71→His	1129	GCACGCTTAGGA***T***GGTAACCGTCCC
Arg71→Lys	2130	GGACGGTTAC***AAG***CCTAAGCGTGCT
Arg71→Lys	1130	GCACGCTTAGG***CTT***GTAACCGTCCC
Ser114→Ala	1134	GGCACTGCCGCGGCTATGGCTTG***C***TTTTGAAGCCACG
Ser115→Ala	1136	GGCACTGCCGCGGCTATGG***GC***TGATTTTGAAGCCACG
Asp142→Ala	2124	CGATTTG***CC***TTTATGGATGAACG
Asp142→Ala	1124	GTTCATCCATAAA***GG***CAAATCGGCTCC
Asp142→Asn	2125	CGATTT***A***A***C***TTTATGGATGAACG
Asp142→Asn	1125	GTTCATCCATAAA***G***T***T***AAATCGGCTCC

Mismatch mutations are bold and italicized.

primers). The resulting PCR-amplified DNA fragments were gel purified and subjected to a second round of PCR using the 2044/1101 primer pair for all mutants except for the Asp142 mutants, in which the PCRs were performed using the 2001/RSRP primer pair. The purified SOE-amplified DNA fragment was digested with *Sac*II and *Hin*dIII for the Asp142 mutants and *Nde*I and *Sac*II for the remaining mutants, gel purified and subcloned into a pIADL14.

Overproduction and purification of the MBP-VanX fusion mutants

Overexpression was performed as described in McCafferty *et al.* [23]. Purification was performed as described previously [17]. The yield of pure MBP–VanX protein obtained from 1 l culture of induced *E. coli* BL21(DE3) cells was ~40 mg.

Protein quantitation and SDS–polyacrylamide gel electrophoresis

Concentration of pure protein was determined by UV–visible spectroscopy and extinction coefficients (ε_{280}, 118,720 $M^{-1}cm^{-1}$ for all mutants, except Tyr21→Phe and Tyr35→Phe for which ε_{280} was 117,230 $M^{-1}cm^{-1}$) were calculated based on a modification of the Edelhoch method [39,40]. Proteins were separated by SDS–PAGE using a discontinuous Tris/glycine buffer [41] with 10% acrylamide resolving gels and 5% acrylamide stacking gels containing 0.1% SDS.

Enzyme activity

Enzyme activity was measured in 50 mM Tris (pH 8.0) at 37°C according to published procedures [14] using the modified cadmium–ninhydrin assay method, which detects the production of free D-Ala [42].

Acknowledgements

We are grateful to Abbott Laboratories for providing the coordinates of the enterococcal VanX crystal structure and particularly to Dirk Bussiere for his input on interpretation of the activity of the mutants proteins. We also thank Roger Flugel for help with the figures generated with the programs GRASP and Quanta and Dewey McCafferty and members of the Walsh laboratory for insightful discussions. I.A.D.L. acknowledges the Medical Research Council of Canada for Postdoctoral Fellowship support. This research was supported in part by a grant from Abbott Laboratories and by NIH GM21643.

References

1. Neu, H.C. (1992). The crisis in antibiotic resistance. *Science* **257**, 1064-1073.
2. Tomasz, A. (1994). Multiple-antibiotic-resistant pathogenic bacteria. A report on the Rockefeller University Workshop. *N. Engl. J. Med.* **330**, 1247-1251.
3. Swartz, M.N. (1994). Hospital-acquired infections: diseases with increasingly limited therapies. *Proc. Natl Acad. Sci. USA* **91**, 2420-2427.
4. Kirst, H.A., Thompson, D.G. & Nicas, T.I. (1998). Historical yearly usage of vancomycin. *Antimicrob. Agents Chemother.* **42**, 1303-1304.
5. Leclercq, R. & Courvalin, P. (1997). Resistance to glycopeptides in enterococci. *Clin. Infect. Dis.* **24**, 545-554.
6. Murray, E. (1997). Vancomycin-resistant enterococci. *Am. J. Med.* **102**, 284-293.
7. Cunha, B.A. (1995). Vancomycin. *Med. Clin. N. Am.* **19**, 817-831.
8. Arthur, M. & Courvalin, P. (1993). Genetics and mechanisms of glycopeptide resistance in enterococci. *Antimicrob. Agents Chemother.* **37**, 1563-1571.
9. Arthur, M., Molinas, C., Depardieu, F. & Courvalin, P. (1993). Characterization of Tn*1546*, a Tn3-related transposon conferring glycopeptide resistance by synthesis of depsipeptide peptidoglycan precursors in *Enterococcus faecium* BM4147. *J. Bacteriol.* **175**, 117-127.
10. Walsh, C.T., Fisher, S.L., Park, I.-S., Prahalad, M. & Wu, Z. (1996). Bacterial resistance to vancomycin: five genes and one missing hydrogen bond tell the story. *Chem. Biol.* **3**, 21-28.
11. Bugg, T.D.H., Wright, G.D., Dutka-Malen, S., Arthur, M., Courvalin, P. & Walsh, C.T. (1991). Molecular basis for vancomycin resistance in *Enterococcus faecium* BM4147: biosynthesis of a depsipeptide peptidoglycan precursor by vancomycin resistance proteins VanH and VanA. *Biochemistry* **30**, 10408-10415.
12. Arthur, M., Molinas, C. & Courvalin, P. (1992). The VanS-VanR two-component regulatory system controls synthesis of depsipeptide peptidoglycan precursors in *Enterococcus faecium* BM4147. *J. Bacteriol.* **174**, 2582-2591.

13. Reynolds, P.E., Depardieu, F., Dutka-Malen, S., Arthur, M. & Courvalin, P. (1994). Glycopeptide resistance mediated by enterococcal transposon *Tn*1546 requires production of VanX for hydrolysis of D-alanyl–D-alanine. *Mol. Microbiol.* **13**, 1065-1070.
14. Wu, Z., Wright, G.D. & Walsh, C.T. (1995). Overexpression, purification, and characterization of VanX, a D-,D-dipeptidase which is essential for vancomycin resistance in *Enterococcus faecium* BM4147. *Biochemistry* **34**, 2455-2463.
15. Reynolds, P.E. (1998). Control of peptidoglycan synthesis in vancomycin-resistant enterococci: D,D-peptidases and D,D-carboxypeptidases. *Cell Mol. Life Sci.* **54**, 325-331.
16. Marshall, C.G., Lessard, I.A.D., Park, I.-S. & Wright, G.D. (1998). Glycopeptide antibiotic genes in glycopeptide-producing organisms. *Antimicrob. Agents Chemother.* **42**, 2215-2220.
17. Lessard, I.A.D. *et al.*, & Walsh, C.T. (1998). Homologs of the vancomycin resistance D-Ala–D-Ala dipeptidase VanX in *Streptomyces toyocaensis*, *Escherichia coli* and *Synechocystis*: attributes of catalytic efficiency, stereoselectivity and regulation with implications for function. *Chem. Biol.* **5**, 489-504.
18. Marshall, C.G. & Wright, G.D. (1997). The glycopeptide antibiotic producer *Streptomyces toyocaensis* NRRL 15009 has both D-alanyl-D-alanine and D-alanyl-D-lactate ligases. *FEMS Micriobiol. Lett.* **157**, 295-299.
19. Bussiere, D.E., Pratt, S.D., Katz, L. Severin, J.M., Holzman, T. & Park, C. (1998). The structure of VanX reveals a novel amino-dipeptidase involved in mediating transposon-based vancomycin resistance. *Mol. Cell* **2**, 75-84.
20. Fan, C., Moews, P.C., Walsh, C.T. & Knox, J.R. (1994). Vancomycin resistance: structure of D-alanine–D-alanine ligase at 2.3 Å resolution. *Science* **266**, 439-443.
21. Dideberg, O., Charlier, P., Dive, G., Joris, B., Frere, J.M. & Ghuysen, J.M. (1982). Structure of a Zn^{2+}-containing D-alanyl–D-alanine-cleaving carboxypeptidase at 2.5 Å resolution. *Nature* **299**, 469-470.
22. Wu, Z. & Walsh, C.T. (1995). Phosphinate analogs of D-,D-dipeptides: slow-binding inhibition and proteolysis protection of VanX, a D-,D-dipeptidase required for vancomycin resistance in *Enterococcus faecium*. *Proc. Natl Acad. Sci. USA* **92**, 11603-11607.
23. McCafferty, D.G., Lessard, I.A.D. & Walsh, C.T. (1997). Mutational analysis of potential zinc-binding residues in the active site of the enterococcal D-Ala–D-Ala dipeptidase VanX. *Biochemistry* **36**, 10498-10505.
24. Park, I.-S., Lin, C.H. & Walsh, C.T. (1996). Gain of D-alanyl–D-lactate or D-lactyl–D-alanine synthetase activities in three active-site mutants of the *Escherichia coli* D-alanyl–D-alanine ligase B. *Biochemistry* **35**, 10464-10471.
25. Shi, Y. & Walsh, C.T. (1995). Active site mapping of *Escherichia coli* D-Ala–D-Ala ligase by structured-based mutagenesis. *Biochemistry* **34**, 2786-2776.
26. Arthur, M., Depardieu, F., Cabanié, L., Reynolds, P. & Courvalin, P. (1998). Requirement of the VanY and VanX D,D-peptidases for glycopeptide resistance in enterococci. *Antimicrob. Agents Chemother.* **36**, 1514-1518.
27. Wright, G.D., Molinas, C., Arthur, M., Courvalin, P., & Walsh, C.T. (1992). Characterization of VanY, a D,D-carboxypeptidase from vancomycin-resistant *Enterococcus faecium* BM4147. *Antimicrob. Agents Chemother.* **36**, 1514-1518.
28. Holden, H.M., Tronrud, D.E., Monzingo, A.F., Weaver, L.H. & Matthews, B.W. (1987). Slow- and fast-binding inhibitors of thermolysin display different modes of binding: crystallographic analysis of extended phosphonamidate transition-state analogues. *Biochemistry* **26**, 8542-8553.
29. Izquierdo-Martin, M. & Stein, R.L. (1992). Mechanistic studies on the inhibition of thermolysin by a peptide hydroxamic acid. *J. Am. Chem. Soc.* **114**, 325-331.
30. Mock, W.L. & Stanford, D.J. (1996). Arazoformyl dipeptide substrates for thermolysin. Confirmation of a reverse protonation catalytic mechanism. *Biochemistry* **35**, 7369-7377.
31. Christianson, D.W. & Lipscomb, W.N. (1989). Carboxypeptidase A. *Accounts Chem. Res.* **22**, 62-69.
32. Mock, W.L. & Zhang, J.Z. (1991). Mechanistically significant diastereoselection in the sulfoximine inhibition of carboxypeptidase A. *J. Biol. Chem.* **266**, 6393-6400.
33. Lipscomb, W.N. & Sträter, N. (1996). Recent advances in zinc enzymology. *Chem. Rev.* **96**, 2375-2433.
34. Sambrook, J. Fritsch, E.F. & Maniatis, T. (1989). *Molecular Cloning: A Laboratory Manual*, 2nd Ed. Cold Spring Harbor Laboratory, Cold Spring Harbor, NY.
35. Saiki, R.K., *et al.*, & Arnheim, N. (1985). Enzymatic amplification of beta-globin genomic sequences and restriction site analysis for diagnosis of sickle cell anemia. *Science* **230**, 1350-1354.
36. Saiki, R.K., *et al.*, & Erlich, H.A. (1988). Primer-directed enzymatic amplification of DNA with a thermostable DNA polymerase. *Science* **239**, 487-491.
37. Lessard, I.A.D. & Perham, R.N. (1994). Expression in *Escherichia coli* of genes encoding the E1α and E1β subunits of the pyruvate dehydrogenase complex of *Bacillus stearothermophilus* and assembly of a functional E1 component (α^2 β^2) *in vitro*. *J. Biol. Chem.* **269**, 10378-10383.
38. Ho, S.N., Hunt, H.D., Horton, R.M., Pullen, J.K. & Pease, L.R. (1989). Site-directed mutagenesis by overlap extension using the polymerase chain reaction. *Gene* **77**, 51-59.
39. Edelhoch, H. (1967). Spectroscopic determination of tryptophan and tyrosine in proteins. *Biochemistry* **6**, 1948-1954.
40. Pace, C.N., Vajdos, F. Fee, L., Grimsley, G. & Gray, T. (1995). How to measure and predict the molar absorption coefficient of a protein. *Protein Sci.* **4**, 2411-2423.
41. Laemmli, U.K. (1970). Cleavage of structural proteins during the assembly of the head of bacteriophage T4. *Nature* **227**, 680-685.
42. Doi, E., Shibata, D. & Matoba, T. (1981). Modified colorimetric ninhydrin methods for peptidase assay. *Anal. Biochem.* **118**, 173-184.
43. Nicholls, A., Sharp, K.A. & Honig, B. (1991). Protein folding and association: insights from the interfacial and thermodynamic properties of hydrocarbons. *Proteins* **11**, 57-68.
44. Thompson, J.D., Higgins, D.G. & Gibson, T.J. (1994). CLUSTAL W: improving the sensibility of progressive multiple sequence alignment through sequence weighting, position-specific gap penalties and weight matrix choice. *Nucleic Acids. Res.* **22**, 4673-4680.

Because *Chemistry & Biology* operates a 'Continuous Publication System' for Research Papers, this paper has been published via the internet before being printed. The paper can be accessed from http://biomednet.com/cbiology/cmb – for further information, see the explanation on the contents pages.